Supporting Information

qNMR fluorine pollution analysis: perspectives on PFAS exposure characterization using ^{19}F NMR

Laura Duciel, Julia Asencio Hernàndez, Marc-André Delsuc, Anne Briot-Dietsch[*]

Corresponding author
Anne Briot-Dietsch
E-mail: anne.briot-dietsch@casc4de.eu

This PDF file includes:

Supporting text
Figs. S1 to S10 Tables ST1 ST2

Fig-S1 Measure of T_1 on PFOA

Inversion Recovery (IR) curve fits to determine longitudinal relaxation time T_1 for different kind of nuclear spins in fluorinated moieties -CH_3 -CH_2 in the PFOA molecule.

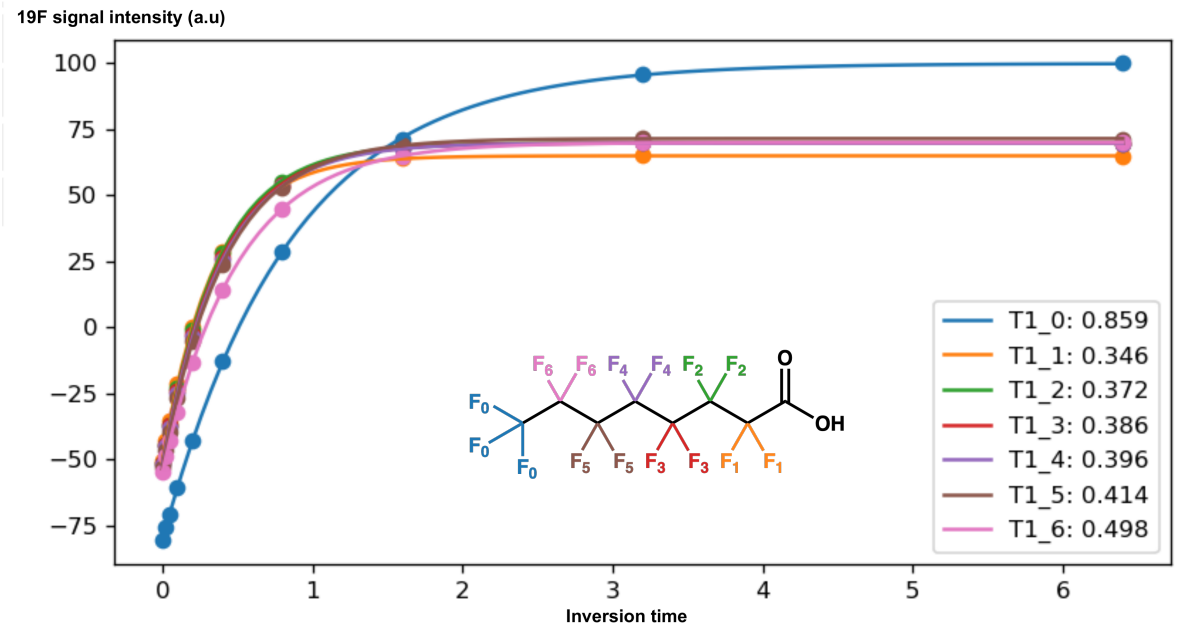


```
1  T1:  0.346 ± 0.0 sec  -  R1: 2.8914 ± 0.0001 sec ¹
2  T1:  0.371 ± 0.0 sec  -  R1: 2.6958 ± 0.0002 sec ¹
3  T1:  0.385 ± 0.0 sec  -  R1: 2.5943 ± 0.0002 sec ¹
4  T1:  0.396 ± 0.0 sec  -  R1: 2.5242 ± 0.0001 sec ¹
5  T1:  0.414 ± 0.0 sec  -  R1: 2.4149 ± 0.0001 sec ¹
6  T1:  0.498 ± 0.0 sec  -  R1: 2.0064 ± 0.0001 sec ¹
0  T1:  0.859 ± 0.0 sec  -  R1: 1.1641 ± 0.0 sec ¹
```

The -CH_2 moiety located alpha to the functional group experiences the fastest longitudinal relaxation at $T_1^1 = 0.346\ s$ and the -CF_3 moiety presents the longest T_1 at $T_1^0 = 0.859\ s$

Computing accuracy and precision,

given the flip angle, as a function of T_1 and the recovery time.

For a given flip angle and a given T_R (recovery time), we can calculate the sensitivity, as a ratio to the full magnetization, and the accuracy computed as the biais against the ideal measure, both expressed in %.

This is performed with the two python functions below `seq()` and `snr()`. The results are given in the tables T1 and T2 below, tabulated for varying T_R/T_1 and for different flip angles, and shown in **Fig-S2** for all possible values of T_R/T_1.

```
"""
these two functions are used to compute the steady magnetisation
and the sensitivity.

These two functions are then used to compute the table and the graphic
for varying value of TR/T1
"""

def seq(flip, Tr, niter=None):
    """
    given flip angle (in °) and Tr recovery time (in multiple of T1)
    it simulates the steady state with n iterations (or 10xT1 if n not given)
    """
    M1 = 1.0
    if niter == None:
        niter = int(10/Tr +1)
    for i in range(niter):
        Mo = M1*m.cos((m.pi*flip)/180) # reste sur z après le pulse
        M1 = 1 - (1 - Mo)*m.exp(-Tr)  # sur z après Tr
    return M1

def snr(flip, Tr):
    """
    in % computed for a total acquisition time of 100 T1
    (as NS is prop to Tr !)
    """
    Mx = seq(flip, Tr)*m.sin(m.pi*flip/180)
    return 100*Mx*m.sqrt(2/Tr)
```

Table ST1

Accuracy in %

for varying pulse flip angle and varying T_R/T_1

	TR/T1	90°	60°	45°	30°	20°
0	0.5	39.347	56.473	68.895	82.883	91.494
1	0.7	50.341	66.970	77.584	88.327	94.385
2	1.0	63.212	77.460	85.437	92.767	96.609
3	1.4	75.340	85.936	91.252	95.799	98.064
4	2.0	86.466	92.742	95.617	97.946	99.065
5	2.5	91.792	95.720	97.448	98.816	99.464
6	3.0	95.021	97.447	98.489	99.303	99.685
7	3.5	96.980	98.467	99.096	99.585	99.813
8	4.0	98.168	99.076	99.457	99.751	99.888
9	5.0	99.326	99.662	99.802	99.909	99.959
10	6.0	99.752	99.876	99.927	99.967	99.985
11	7.0	99.909	99.954	99.973	99.988	99.994
12	8.0	99.966	99.983	99.990	99.996	99.998
13	9.0	99.988	99.994	99.996	99.998	99.999
14	10.0	99.995	99.998	99.999	99.999	100.000

Table ST2

Relative sensibility in %

for varying pulse flip angle and varying T_R/T_1

	TR/T1	90°	60°	45°	30°	20°
0	0.5	78.69	97.81	97.43	82.88	62.59
1	0.7	85.09	98.03	92.73	74.65	54.57
2	1.0	89.40	94.87	85.44	65.60	46.73
3	1.4	90.05	88.95	77.12	57.25	40.09
4	2.0	86.47	80.32	67.61	48.97	33.88
5	2.5	82.10	74.14	61.63	44.19	30.43
6	3.0	77.58	68.91	56.86	40.54	27.84
7	3.5	73.31	64.46	52.97	37.64	25.81
8	4.0	69.42	60.67	49.73	35.27	24.16
9	5.0	62.82	54.59	44.63	31.59	21.62
10	6.0	57.59	49.94	40.80	28.86	19.74
11	7.0	53.40	46.27	37.79	26.72	18.28
12	8.0	49.98	43.29	35.35	25.00	17.10
13	9.0	47.13	40.82	33.33	23.57	16.12
14	10.0	44.72	38.73	31.62	22.36	15.30

From these tables, for a given sample, we consider

- the molecule's longest T_1 : T_1^M.
- the acceptable error rate

then choose in table ST1 the T_R/T_1 line where this error rate is found, either at 90° or at a lower angle $\Rightarrow$ this determines $\alpha = T_R/T_1$

Finally, given an acquisition time AQ one can set $D1$ such that $T_R = D1 + AQ = \alpha \times T_1^M$.

Fig-S2 Graphical output

Accuracy and Relative sensitivity, expressed in % for different pulse flip angle versus T_R/T_1

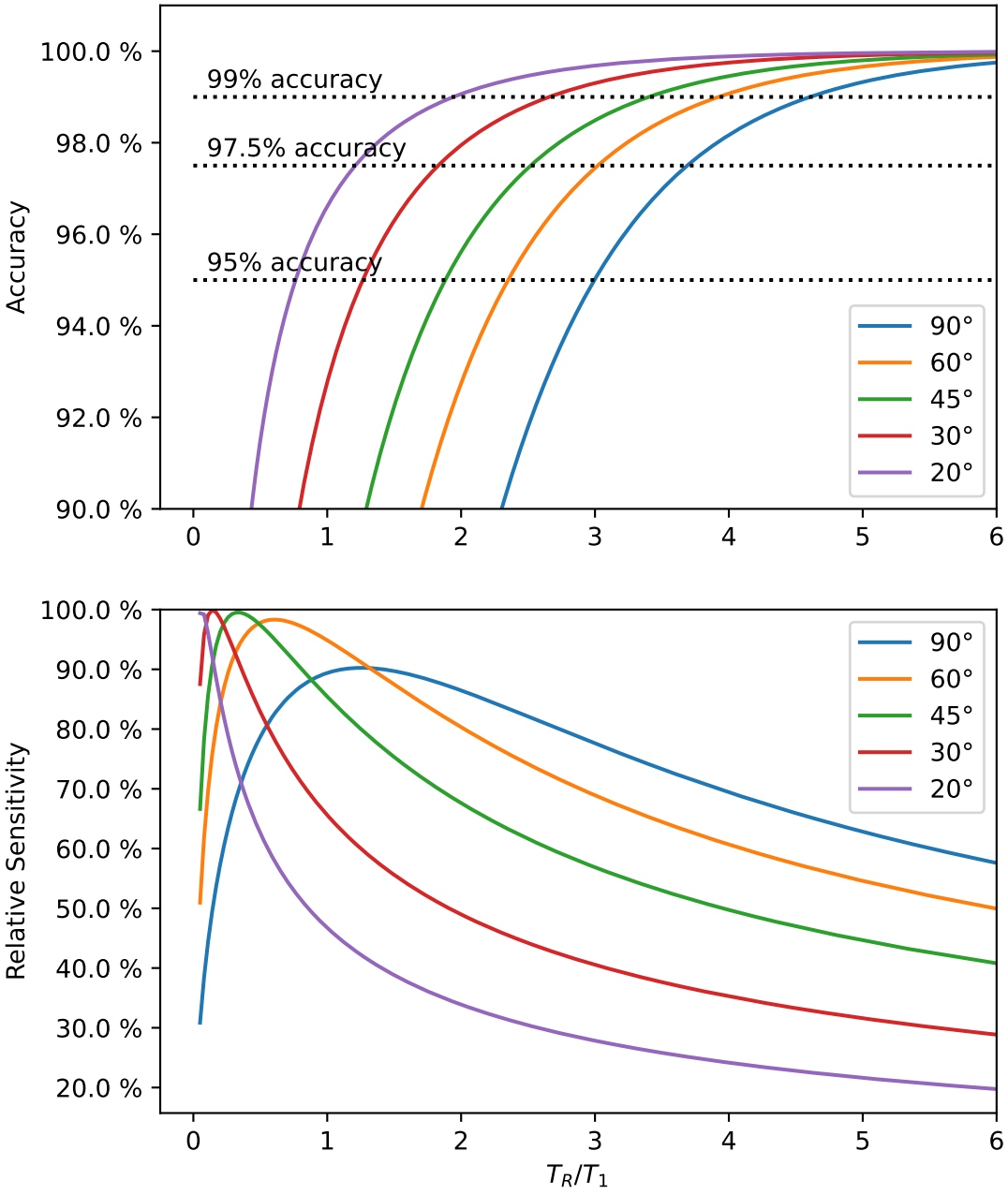

Robustness of the OPERA-45 sequence vs miss-calibration

Fig-S3 Power miss-calibration

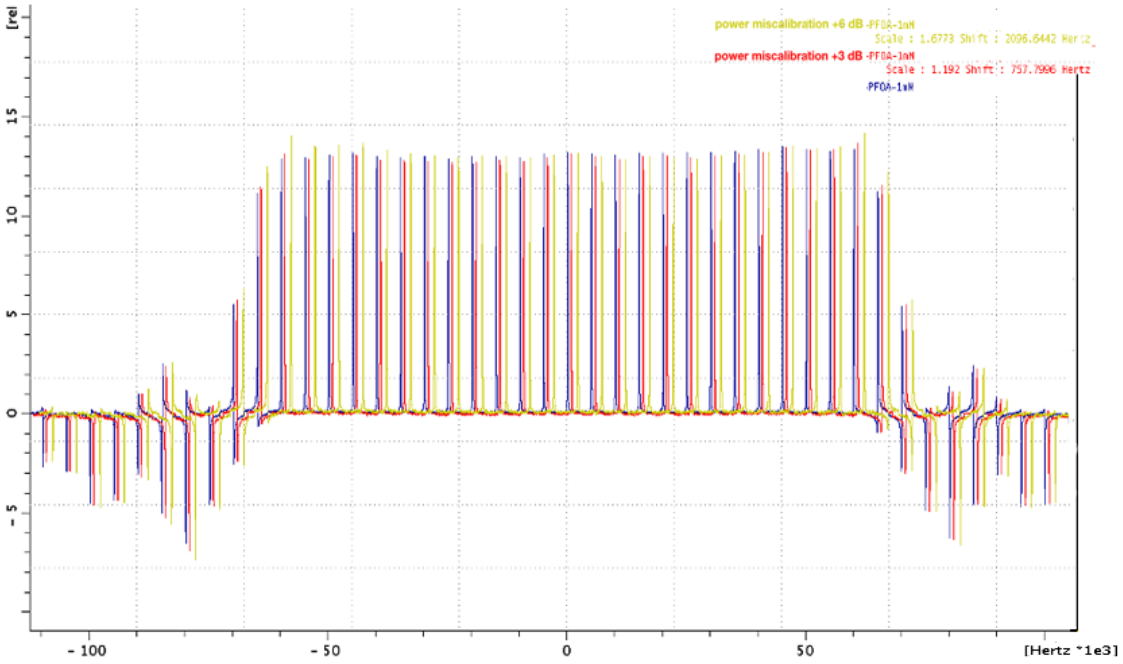

Experimental excitation profile measured by moving the carrier frequency of the OPERA-45 pulse on a 1mM PFOA sample in DMSO in optimized conditions, measure on the -CF_3.

- **blue**: calibrated pulse
- **red**: 3 dB miss-calibration of the B_1 field *(30% error on the B_1 amplitude)*
- **green**: 6 dB miss-calibration of the B_1 field *(50% error on the B_1 amplitude)*

The excitation remains consistent across a 100 kHz range of frequencies, with fluctuation that do not exceed 1.5% in intensity for the 3 dB missmatch and 3.5% for the 6 dB missmatch. No phase distortion is observed in the 100 kHz spectral range.

2D PULSE SEQUENCES

Here we present graphically the various NMR pulse sequences used in this study.

Fig-S4 ^{19}F-DOSY

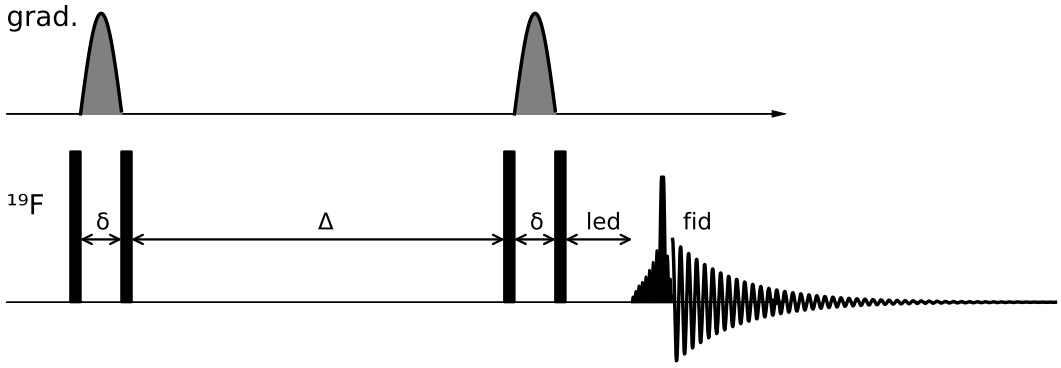

The ^{19}F-DOSY is based on the standard led [1] pulse sequence, with only the last reading pulse modified to incorporate the OPERA-45 pulse. The spectral width is thus limited by the 4 strong pulses. These should be 90° pulses, but shorter values can be used to extend the spectral range, with the difficulty of weakening the resulting signal.

In this experiment, all delays are kept constant, and the Pulsed Fielf Gradients (PFG) are varied in intensity, ranging from vanishing small to maximum intensities.

[1] Gibbs SJ, Johnson CS. A PFG NMR experiment for accurate diffusion and flow studies in the presence of eddy currents. *J.Magn.Res.(1969)* 1991; **93**(2):395–402. doi:10.1016/0022-2364(91)90014-k

Fig-S5 ^{19}F DOSY

A calibration DOSY spectrum was acquired on a mix made in purpose, composed of PFMOPrA (MW=230D), TFE(MW=100D), and PFOS (MW=500D). Acquisition was performed using 32 gradients linearly sampling from 0.48 to 47.19 G/cm for a total time of 37 minutes. A Laplace transform of performed using the PALMA algorithm[2], with a Laplace window of 50 to 5000 $\mu m^2/s$, $\lambda = 0.01$ and 10,000 iterations. The result is shown below.

Measured diffusion coefficients are TFE: $720 \pm 15 \mu m^2/s$, PFMOPrA: $553 \pm 20 \mu m^2/s$, and PFOS: $488 \pm 25 \mu m^2/s$.

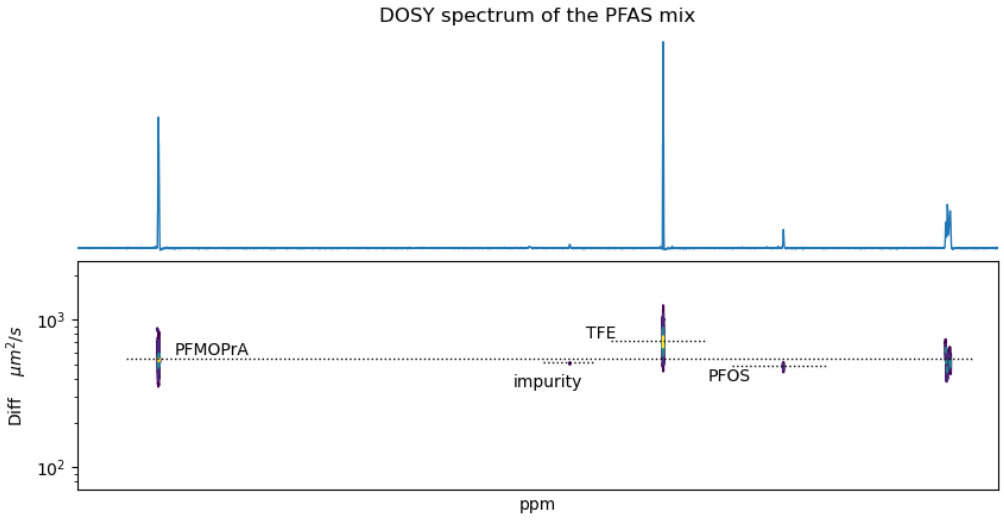

[2]PALMA, an improved algorithm for DOSY signal processing. Cherni A., Chouzenoux É., Delsuc M-A. (2017) *Analyst* **142** p772–779. doi:10.1039/C6AN01902A

Fig-S6 ^{19}F-^{19}F COSY45

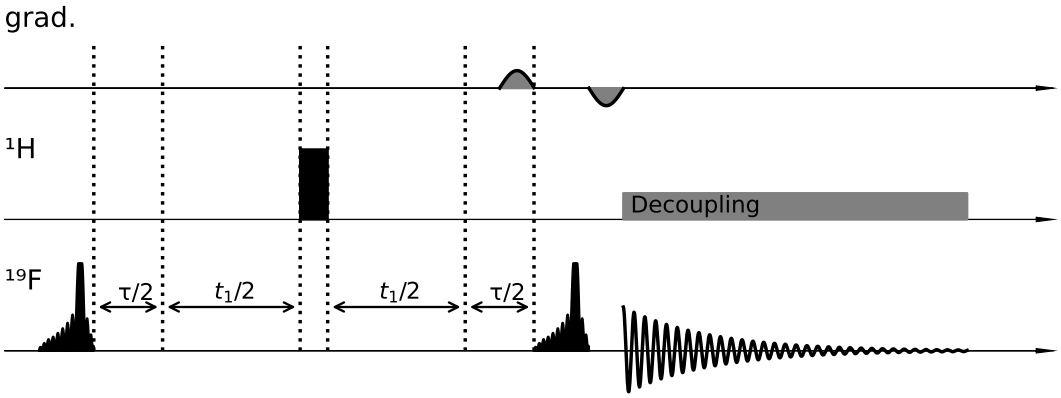

The ^{19}F-COSY-45 is nearly similar to the standard COSY-45 experiment[3], except for the initial pulse which is also an OPERA-45

In order to enhance the signal-to-noise on ^{1}H-coupled ^{19}F molecules, a ^{1}H decoupling was added to the sequence by a broad-band decoupling during acquisition and a 180° ^{1}H pulse in the middle of the t_1 ^{19}F evolution. The delay τ allows the weaker J-couplings to be expressed as correlation peaks. This is particularly useful, considering the very large F1 spectral width, implying short increments, and the limited number of increments.

Two versions of the coherence transfer pathways are possible: the standard anti-echo experiment with the two PFGs having inversed intensity, as presented here; and the echo experiment with both PFGs being equivalent.

[3]A. BAX and R. FREEMAN. *J.Magn.Reson.* **44**, 542 (1981)

Fig-S7 ^{19}F COSY-45 of Vertrel

The COSY-45 was measured on the same 2H,3H-decafluoropentane sample than the HMQC (see text). Each fid was acquired with a 100 kHz spectral width (177.11 ppm), with the Digital filtering set to smooth, on 16 k points and a 1.85 s relaxation delay. The ^{19}F excitation pulse was the same OPERA-45 pulse as used in other experiments. The ^{1}H refocusing pulse had a duration of 24μs. The gradients had a value of 15 G/cm and a 1 ms duration sine-bell shape. The $\tau/2$ value was chosen at 6.35 ms. Four scans were acquired per increment and 2048 increments were performed for a total acquisition time of 4h 30min.

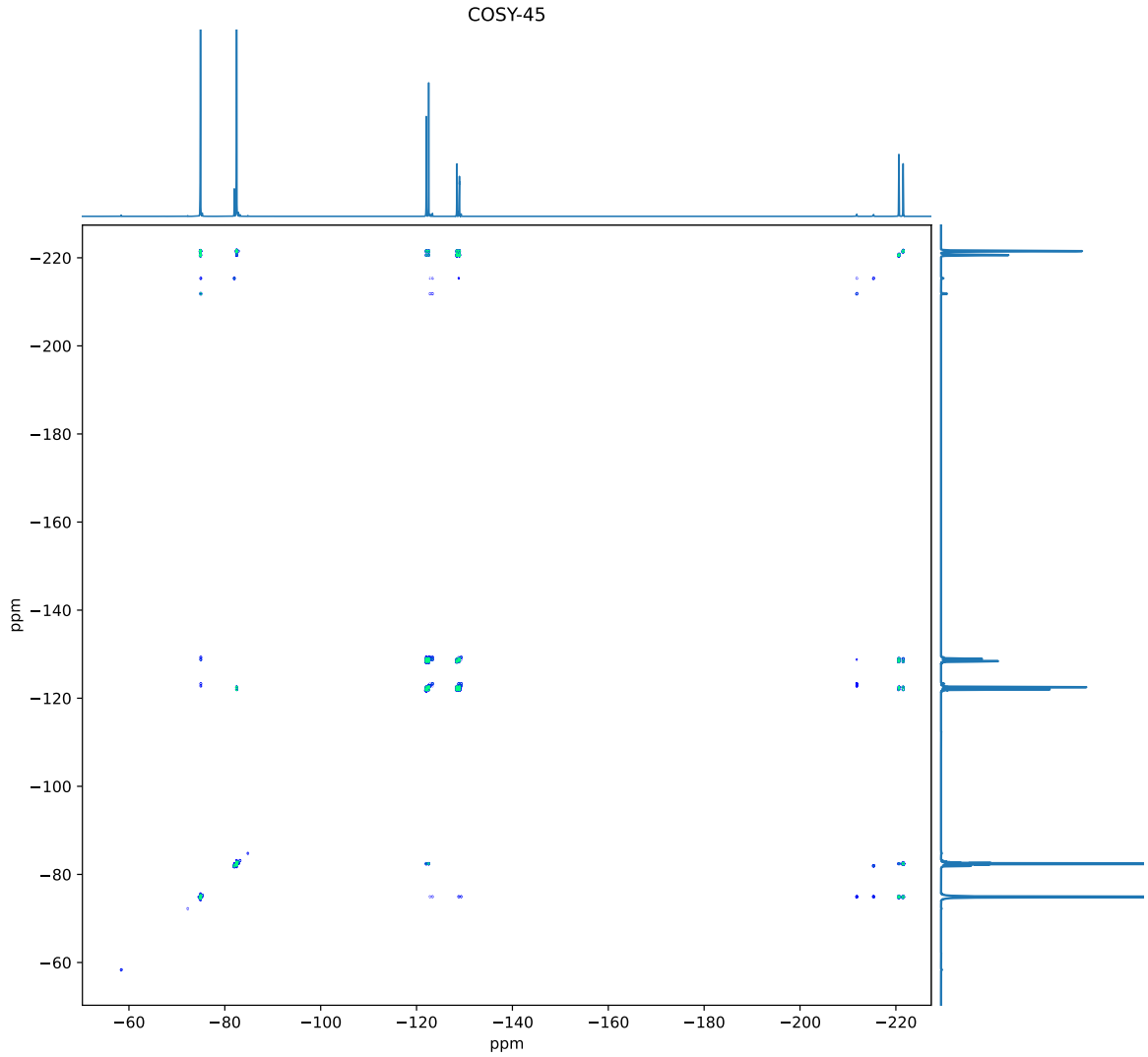

The Broad-Band COSY-45 of the Vertel product

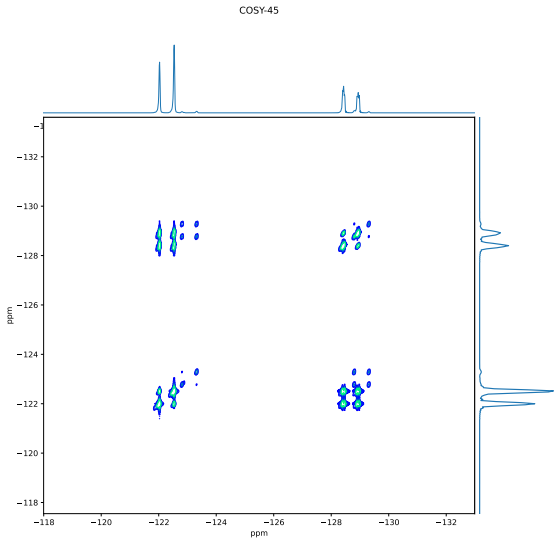

Zoom showing the major and minor forms

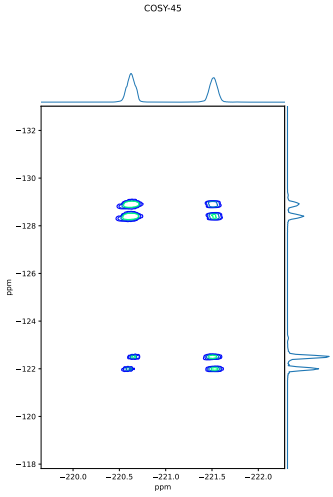

Zoom showing the 45° effect

Fig-S8 ^{19}F COSY-45 of PFOA

A high resolution COSY-45 expermient was performed on PFOA (Per Fluorinated Octanoic Acid). The experiment was performed on 100kHz spectral width on both axes, with 16k points acquisition and 8k increments. Processing was performed in magnitude with sine-bell apodisation and no zerofilling.

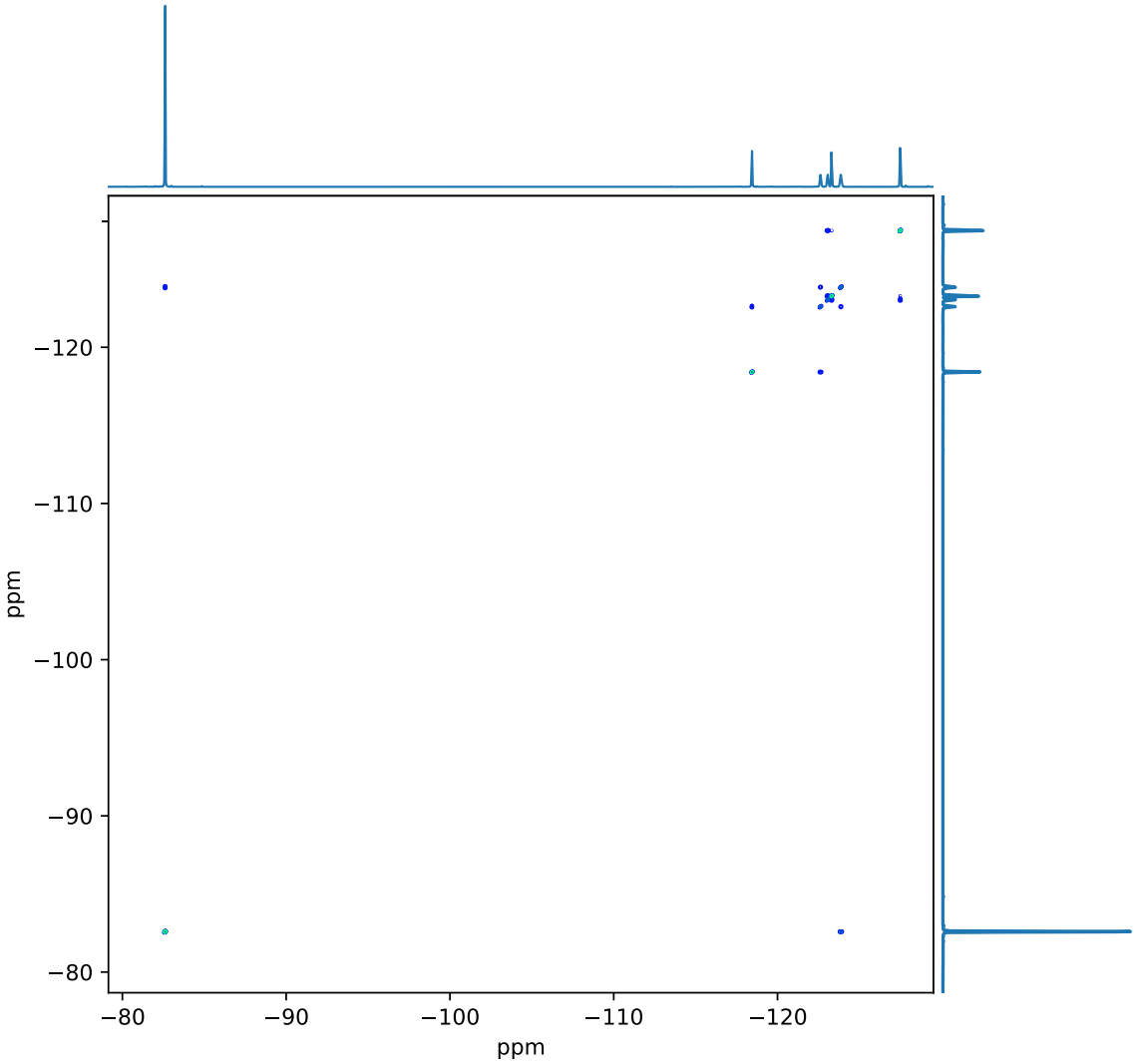

The COSY-45 of PFOA

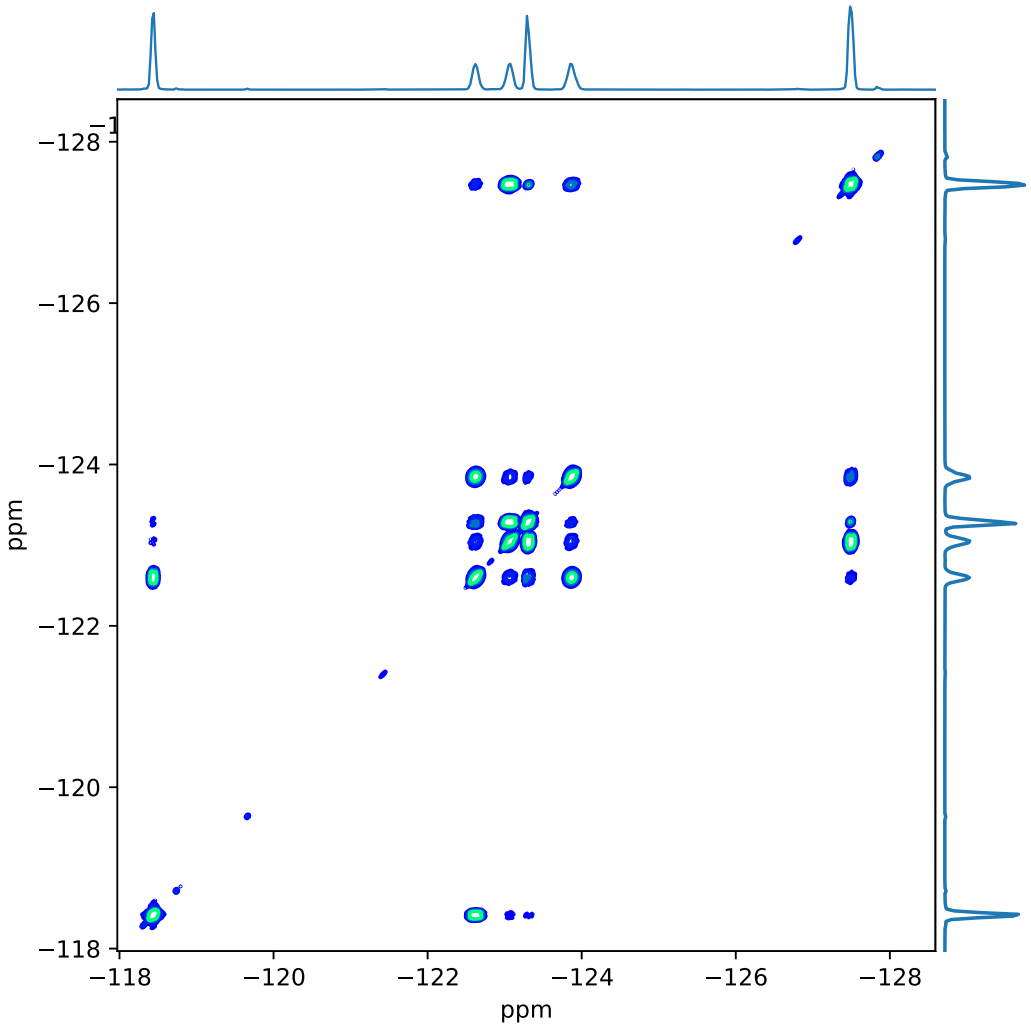

Zoom of the CF_2 region at a lower level, showing the long range couplings

Fig-S9 ^{19}F-^{13}C sofast-HMQC

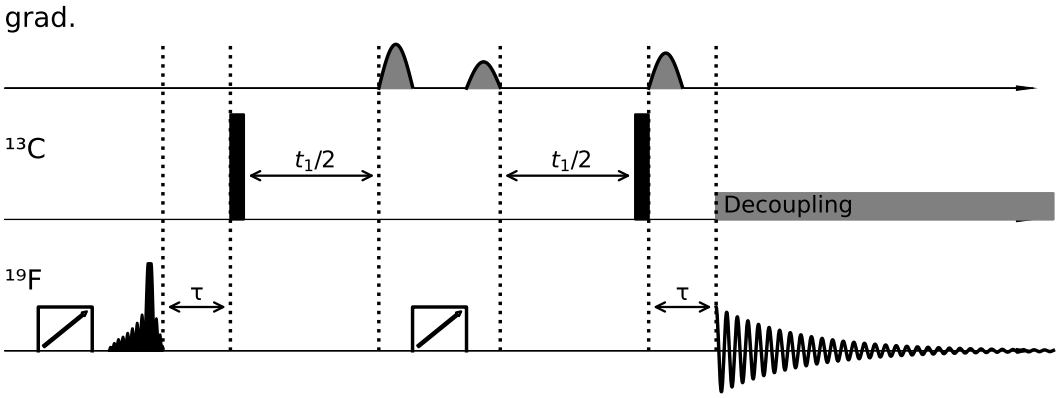

The HMQC sequence contains one excitation pulse implemented here with OPERA-45 and a refocusing pulse implemented here as a frequency swept (chirp) pulse of 1.5 msec duration. The τ delay allows to select a range of ^{19}F-^{13}C J-couplings to be observed, we chose $\tau = \frac{1}{2J}$ with $J = 350$ Hz.

The sofast version[4] of the experiment uses a specific excitation pulse to improve the magnetisation steady state, which is implemented here with another chirp pulse just before the excitation pulse.

The three selection PFG were implemented with the following intensities of 50%, 30%, 41.27%

[4]Schanda,P.; Kupče,E.; Brutscher,B. *J.Biomol.NMR* 2005, **33**, 199-211

Fig-S10 ^{19}F-^{13}C sofast-HMQC of PFOA

A so-fast HMQC expermient was performed on PFOA. The experiment was performed with spectral widthes of 100 kHz on ^{19}F axis, and 25 kHz for ^{13}C (165 ppm) The experiment was run in 4 scans, with 2k points acquisition and 368 increments, for a total acquisition time of 50 min. Processing was performed in magnitude with sine-bell apodisation and no zerofilling.

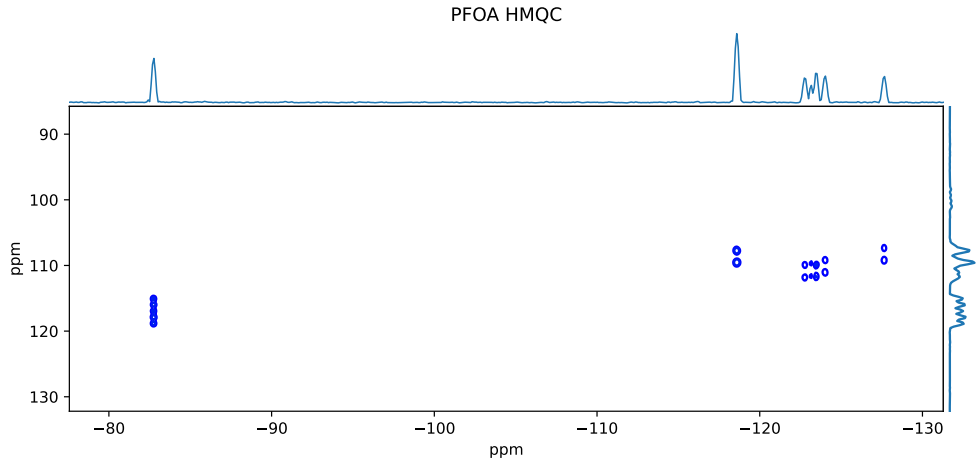

The so-fast HMQC of PFOA

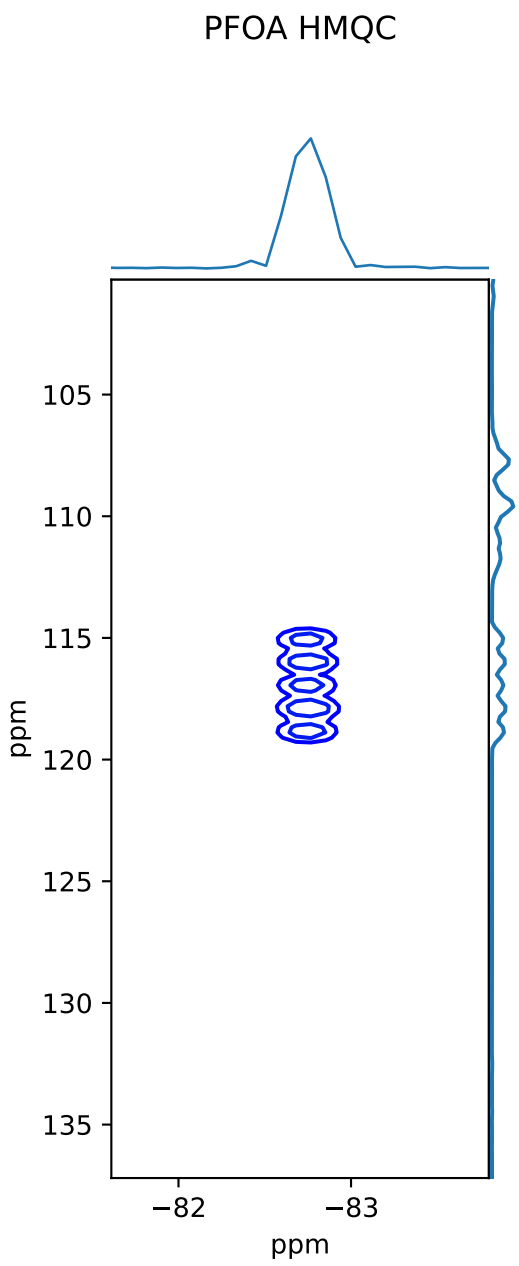

Zoom on the CF_3 region

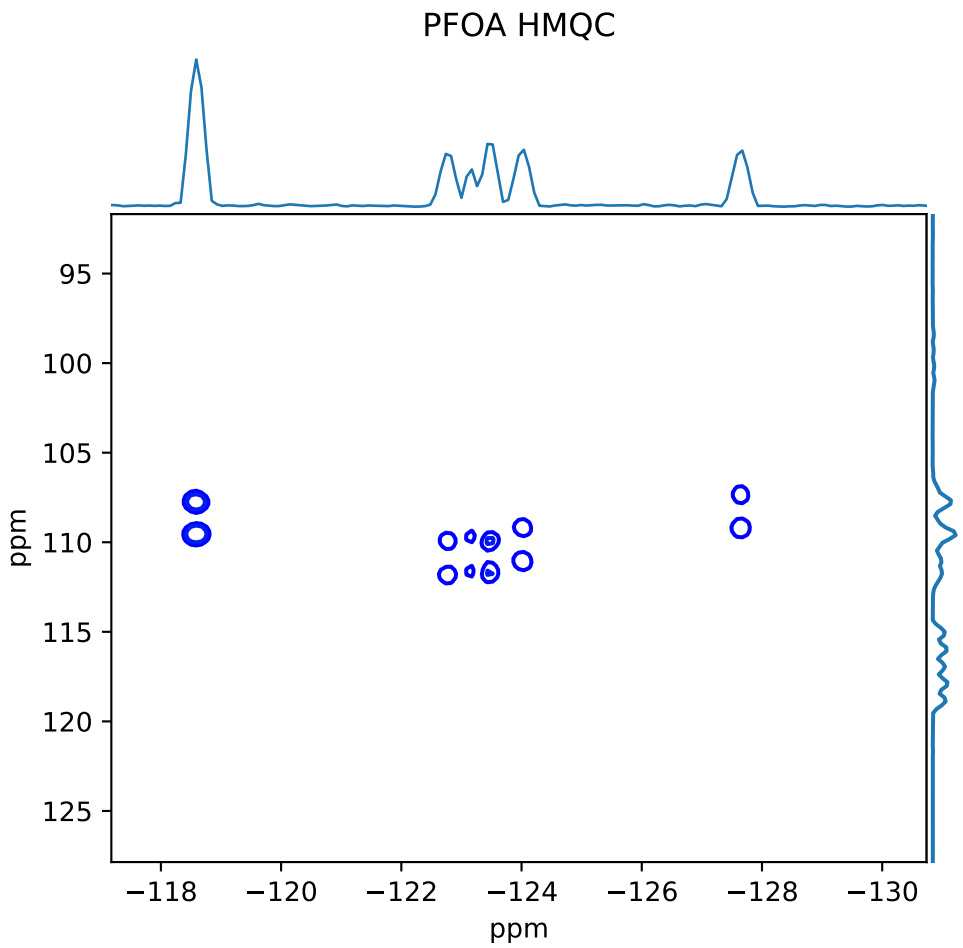

Zoom on the CF_2 region

Fig-S11 ^{19}F Spectra of commercial toothpastes

Spectra of commercial toothpastes illustrating different formulations with fluoride-based additives used to prevent tooth decay, including sodium fluoride (NaF), sodium monofluorophosphate (Na_2PO_3F), stannous fluoride (SnF_2), and Olaflur, an alkyl-ammonium fluoride. These common additives reflect different strategies for enamel strengthening, caries prevention, and oral health maintenance, depending on the formulation's specific goals

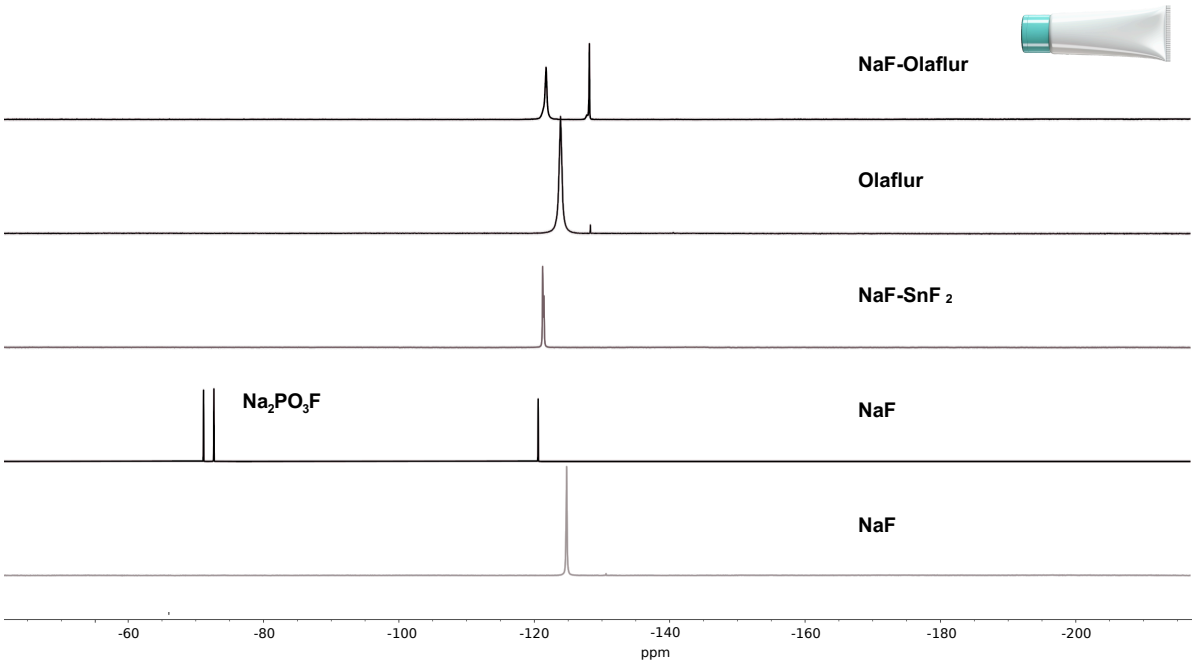
NaF-Olaflur
Olaflur
NaF-SnF 2
Na2PO3F
NaF
NaF
-60
-80
-100
-120
-140
-160
-180
-200
ppm